



## TRANSIENT MATHEMATICAL MODEL FOR WELL KICK DURING DRILLING OPERATIONS

Jonathan Felipe Galdino<sup>1</sup>  
Gabriel Merhy de Oliveira<sup>2</sup>  
Admilson T. Franco<sup>3</sup>  
Cezar O. R. Negrão<sup>4</sup>

Thermal Science Laboratory (LACIT) Post-graduate Program in Mechanical and Materials Engineering (PPGEM), Federal University of Technology - Parana (UTFPR) – Av. Sete de Setembro, 3165, CEP 80.230-901 – Curitiba-PR-Brazil

<sup>1</sup>jonathangrag@gmail.com, <sup>2</sup>gabrielm@utfpr.edu.br, <sup>3</sup>admilson@utfpr.edu.br, <sup>4</sup>negrao@utfpr.edu.br

**Abstract.** An important task during well drilling in deep water is the control of the bottomhole pressure within a narrow range. Whenever the bottomhole pressure becomes smaller than the formation pressure there is a risk of formation fluid invasion (oil, natural gas and/or water) into the wellbore. The influx of the formation fluid to the wellbore, named called kick, can escalate to a blowout if not controlled when the formation fluid reaches the surface. Therefore, a small inflow of gas should be detected as soon as possible. Nevertheless, the pressure is only measured while drilling and also a small influx of gas cannot change significantly the bottomhole pressure. Another indication of kick is the change of pressure at the wellhead which is only noticed when a large amount of gas has invaded the well. The current work presents a compressible transient flow model to predict pressure transmission within the wellbore when a gas influx occurs. The model comprises the conservation equations of mass and momentum which are solved by the method of characteristics. In this first work, drilling fluids are admitted to behave as Newtonian fluid and the viscous effect is modeled by employing a friction factor approach. The influx of gas is defined as a function of the rock permeability and the pressure difference between the reservoir and the well. Model results show that the pressure variation along the time depends on the pressure wave propagation. It can be anticipated that the more viscous the drilling fluid and higher the reservoir permeability, the faster the steady-state pressure is reached after the well has been closed.

**Keywords:** Gas influx, kick, drilling fluid, compressible flow, transient simulation.

### 1. INTRODUCTION

In oil well drilling, the bottomhole pressure must be kept within a narrow range in order to avoid formation damage and/or invasion of formation fluid into the wellbore. Nowadays, the downhole pressure is controlled by balancing the drilling fluid hydrostatic pressure with the formation pressure. Whenever the bottomhole pressure becomes smaller than the formation pressure there is a risk of the formation fluid (oil, natural gas and/or water) come into the wellbore and up to the annulus (the space between the drill string and the walls of the open hole). The influx of the formation fluid is called kick and, if it is not controlled, can escalate to a blowout (the uncontrolled release of crude oil and/or gas from an oil well after pressure control systems have failed) when the formation fluid reaches the surface, especially in case of gas influx. Kick is usually detected by comparing the fluid pumping rate with the returning flow rate to the reservoir. This method, however, allows kick detection only when a significant amount of gas has entered the well which sometimes can be too late to avoid a blowout. Therefore, a small inflow of gas should be detected as soon as possible assuring safety to drilling.

As formation pressure must be higher than the pressure within the wellbore to a kick take place, there must be a sudden pressure change at the well bottom as soon as a small amount of gas has come into the well. The sooner this pressure is sensed the better. Nevertheless, the pressure is only measured while drilling and also a small amount of gas changes slightly the absolute measured pressure.

One of the first models for prediction of kick was proposed by LeBlanc and Lewis (1968) which was improved by Records (1972) by adding head loss in the annular space. A robust model that considers the fluid as Bingham and the gas is assumed disperse in the fluid was developed by Stanbery (1976). In 1981, Hoberoch e Stanbery (1981) elaborated a dynamic model to evaluate the pressure distribution in the annular space assuming single phase flow. A mathematical model to simulate the two-phase flow slippage was proposed by Santos (1982). Nickens (1987), on the other hand, developed a quite complete model for kick simulation which also included several geometric components. A mathematical model to predict the pressure variation in the choke line and in the annular space was proposed by Negrão (1989). The first disperse two-phase flow transient model was brought about by Lage (1990). Ohara (1995) evaluated the effect of gas reservoir, choke line and gas speed. A comparison between different models was conducted by Nunes (2001). Nunes (2001) also developed a model for gas kick simulation in order to compute pressure change in the choke line and annular space for applications in deep and ultra-deep water. Several effects were investigated, such as, pit gain, water depth, drilling fluid density, rheology and flow rate. A similar discussion is undertaken in Nunes *et al.* (2002).

The kick model proposed by Avelar *et al.* (2009) included two-phase flow slippage, pressure loss, a two-parameter rheology model and reservoir coupling. The solution is based on the finite difference method and their results were compared with experimental deep-water well measurements.

Mathematical modeling, on the other hand, can be used to help on the understanding of the problem. Not only should the influx of fluid into the well be modeled but also the complex transient pressure transmission phenomenon that take place in the drilling fluid. A similar case investigated by the literature (Sestak *et al.*, 1987, Cawkwell and Charles, 1987, Chang *et al.*, 1999 and Davidson *et al.*, 2004, Oliveira *et al.*, 2010, Negrão *et al.*, 2011, Vinay *et al.*, 2006, Vinay *et al.*, 2007, Wachs *et al.*, 2009 and El-Gendy *et al.*, 2012) is the flow start-up of viscoplastic materials. Most of the works dealt with the development of mathematical models that simulates the restart of either drilling fluids or waxy crude oils in pipelines. Oliveira *et al.* (2013), for instance, studied the transient flow occurring inside the drill pipe and annular space. The drilling fluid was considered as a non-Newtonian Bingham fluid and the flow is modeled as compressible by using the balance equations of mass and momentum. Comparisons of the mathematical model results of Oliveira *et al.* (2013) with experimental data obtained from a Petrobras experimental rig showed good agreement.

The current study, based on Oliveira's *et al.* (2013) work, proposes a mathematical model for the influx of gas and pressure changes at the well bottom during a gas kick. As soon as the kick is detected, flow circulation is interrupted and the well is closed in order to evaluate pressure variations up to the stabilization. The model is based on the balance equations of mass and momentum that are discretized by the Method of Characteristics. The flow is considered laminar, isothermal, compressible and one-dimensional and the fluid is treated as Newtonian. The shear stress is assumed to change linearly across the pipe cross section. At this moment, the migration and dissolution of the gas are disregarded and the focus of this study is the drilling fluid volume gain on the surface and time required to stabilize the pressure after the well be closed.

## 2. MATHEMATICAL MODEL

### 2.1. Problem description

Figure 1a shows a schematic representation of the drilling operation at the wellbore bottom in which a drilling fluid is pumped into the drill pipe. The fluid flows through the drill bit roles and then returns to the surface by the annular space carrying the cuttings. Despite the changes of the cross sectional areas of the drill pipe and annular space, the geometry will be simplified as a constant cross sectional drill pipe and annular space, as shown in Figure 1b. According to Figure 1c, the drill pipe internal diameter is identified as  $D$  and the internal and external diameters of the annular space as  $D_1$  and  $D_2$ , respectively. The region below the drill pipe is disregarded in the modeling and the fluid is considered to flow directly from the drill pipe to the annular space, as the drill bit is not considered to be in place.

At the problem start-up, a formation region with a pressure higher than the bottom pressure is hit while drilling and an influx of gas begins to take place. After a certain amount of gas had entered the well, drilling fluid pumping is stopped and the well is suddenly closed in order to avoid a blowout.

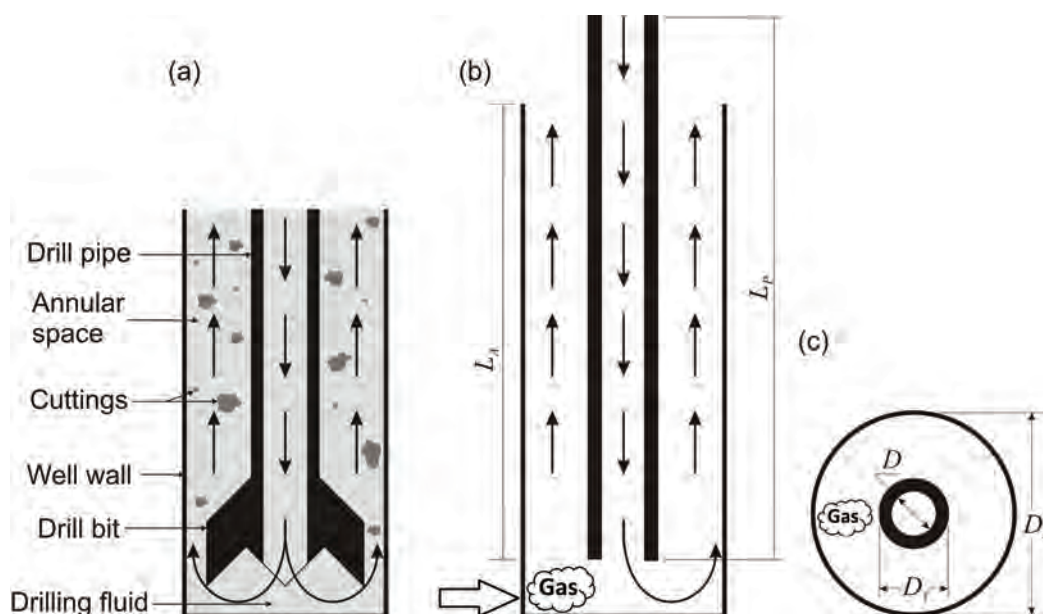


Figure 1. (a) Illustration of the drilling fluid circulation in the wellbore. (b) Longitudinal view and (c) cross section of drill pipe and annular space

## 2.2 Balance equations

The flow in both drill pipe and annular space is admitted to be compressible, isothermal and one-dimensional in the axial direction. Besides, the drill pipe and the well structure are admitted to be completely rigid and therefore, not deformable. The shear stress variation across the circular geometry (drill pipe and annular space) is admitted constant and the shear stress at the pipe wall is evaluated by employing the concept of friction factor. For this first work, the drilling fluid is considered as Newtonian with constant viscosity and the formation gas as ideal.

The flow is regarded as one-dimensional, laminar and weakly compressible. By using a constant isothermal compressibility,  $\alpha = \frac{1}{\rho} \left( \frac{\partial \rho}{\partial P} \right) = \frac{1}{\rho c^2}$ , the mass and momentum conservation equations can be written, respectively, as,

$$\frac{\partial P}{\partial t} + \rho c^2 \frac{\partial V}{\partial z} = 0 \quad (1)$$

$$\frac{\partial V}{\partial t} + \frac{1}{\rho} \frac{\partial P}{\partial z} + \frac{2fV|V|}{D_h} + g_z = 0 \quad (2)$$

where  $\rho$ ,  $V$  and  $P$  are the average values of density, velocity and pressure across the cross sectional area and  $c$  is the pressure wave speed.  $f$  is the Fanning friction factor which depends on the geometry (pipe or annular space) and fluid properties.  $t$  is the time and  $z$  is the axial position.  $D_h$  is the hydraulic diameter, which is defined as  $D_2 - D_1$  for the annular space and  $D$  for the pipe.  $g_z$  is the acceleration of gravity in axial direction.

The friction factor depends on the fluid properties and on the geometry under analysis. For Newtonian laminar flows, Fanning friction factor can be written as (White, 2003):

$$f = \frac{16\zeta}{\text{Re}_{z,t}} \quad (3)$$

where  $\zeta$  is geometric parameter, which is 1.0 for pipe flow and given by Eq. (4) for annular flow, and  $\text{Re}_{z,t}$  is the Reynolds number that depends on time and on the position along the domain ( $\text{Re}_{z,t} = \rho V D_h / \mu$ ).

$$\zeta = \frac{(1-\varepsilon)^2}{1 + \varepsilon^2 - (1-\varepsilon^2)/\ln(1/\varepsilon)} \quad (4)$$

with  $\varepsilon = D_1/D_2$ . The formation gas is admitted as ideal so that,

$$P_g \nabla = mRT \quad (5)$$

where  $P_g$  is the gas absolute pressure,  $m$  is the mass of gas,  $R$  is the specific gas constant,  $T$  is the absolute pressure and  $\nabla$  is the volume occupied by the gas within the wellbore.

The gas that flows to the well is assumed to stay stationary within the borehole and also that is not soluble in the drilling fluid. The influx of gas is determined by using the Darcy's law (Nield and Bejan, 2013), based on the ideal gas properties, on the media permeability and on the pressure difference between the reservoir and the well bottom, so that:

$$Q_g = \frac{kA_r(P_r - P_w)}{\mu_g L_r} \quad (6)$$

where  $Q_g$  is the flow rate of gas,  $k$  is the rock permeability,  $P_r$  is the reservoir pressure,  $P_w$  is the pressure within the borehole,  $\mu_g$  is the gas viscosity,  $A_r$  is the reservoir cross section area that is open to the flow,  $L_r$  is the porous media length.

## 2.3 Solution of the equations

The governing equations are solved by the method of characteristics (MOC) that is typically used for solving hyperbolic partial differential equations (see Wylie *et al.*, 1993). The method consists of simplifying partial differential equations to a family of ordinary differential equations, along which the solution can be integrated from an initial condition. In the current case, Eqs. (1) and (2) are reduced to two total differential equations, which are valid over the characteristic lines  $dz/dt = \pm c$ . In as much as  $c$  is constant, plots of  $dz/dt$  provides straight lines on the  $z-t$  plane, such as  $C^+$  and  $C^-$  in Fig. 2a. In order to solve numerically the equations, both length of drillpipe and annular space ( $L_P + L_A$ ) are

divided into  $N$  equal reaches,  $\Delta z$ , as shown in Fig. 2a, and the time-step is computed according to  $\Delta t = \Delta z/c$ . If  $P$  and  $V$  are both known at position  $i-1$  and  $i+1$ , the ordinary differential equations can be integrated over the characteristic line  $C^+$  and  $C^-$ , respectively, and therefore, be written in terms of unknown variables  $P$  and  $V$  at point  $i$ . By solving the two resulting algebraic equations,  $P$  and  $V$  can be obtained at point  $i$  as a function of known values at points  $i-1$  and  $i+1$ :

$$P_i = \frac{F_+ G_- + F_- G_+}{G_+ + G_-} \tag{7}$$

$$V_i = \frac{F_+ - F_-}{G_+ + G_-} \tag{8}$$

where  $F_+ = P_{i-1} + (\rho c - R_+)V_{i-1} - \rho g \Delta z$ ,  $F_- = P_{i+1} - (\rho c - R_-)V_{i+1} + \rho g \Delta z$ ,  $G_+ = \rho c + R_+$ ,  $G_- = \rho c + R_-$ ,  $R_+ = \frac{16\zeta_{i-1}\mu\Delta z}{(D_h^2)_{i-1}}$

and  $R_- = \frac{16\zeta_{i+1}\mu\Delta z}{(D_h^2)_{i+1}}$ . Note that  $P_i$  and  $V_i$  are evaluated as a function of known values at the previous time-step.

In the wellbore bottom, where the gas injection takes place, the domain is discretized according to the scheme of Fig. 2b. Because gas injection at  $t=0$ , the volume occupied by the gas starts to increase as the gas flow,  $Q_g$ , enters the borehole. By using the nomenclature of Fig. 2b, the following characteristic equations  $C^-$  can be written for the pipe ( $s=p$ ) and for the annular space ( $s=a$ ), respectively,

$$C^-(\text{drillpipe}): \quad P_{p,i} = F_- + (\rho c + 16\mu\Delta z/D_{p,i}^2)V_{p,i} \tag{9}$$

$$C^-(\text{annular}): \quad P_{a,i} = F_- + (\rho c + 16\zeta\mu\Delta z/D_{h,a,i}^2)V_{a,i} \tag{10}$$

where the first subscript refers to the domain (drillpipe or annular space) and the second to  $i$  position in the domain.  $F_-$  is computed as a function of known parameters at the previous time-step and  $i=2$  for each domain.

Note that both drillpipe and annular space domains have their origin at the well bottom, so that  $i=1$  for both.

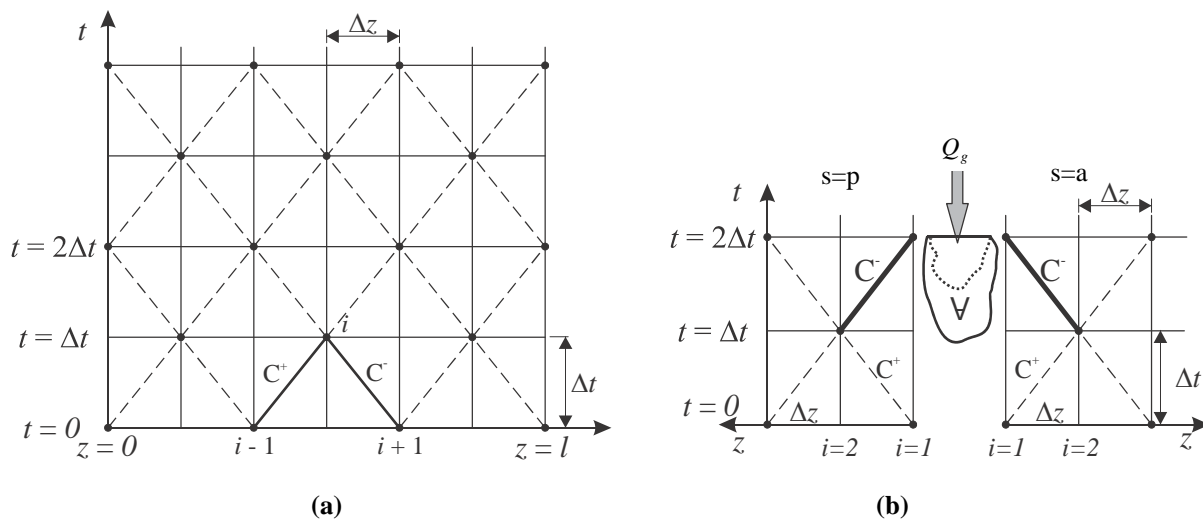


Fig. 2. (a)  $z$ - $t$  grid for solving the governing equation. (b) grid distribution near the well bottom.

By applying the discretized mass balance equation within a time-step length of  $2\Delta t$  to the mass of gas entering the borehole and to the volume of liquid within the well, the mass and the volume of gas can be computed at each time-step. The substitution of these discretized equations into Eq. (5) provides an equation for evaluation of pressure at the borehole bottom:

$$P_g^{t+2\Delta t} = \frac{\left[ m^t + 2\Delta t \frac{(\dot{m}_g^t + \dot{m}_g^{t+2\Delta t})}{2} \right] RT}{V^t + 2\Delta t \left[ \frac{Q_{out}^t + Q_{out}^{t+2\Delta t}}{2} - \frac{(Q_{in}^t + Q_{in}^{t+2\Delta t})}{2} \right]} \tag{11}$$

where  $P_g^{t+2\Delta t}$  is the gas absolute pressure at the borehole bottom at  $t + 2\Delta t$ ,  $m'$  is the mass of gas within the wellbore at time  $t$ ,  $\dot{m}_g$  is the gas mass flow rate to the wellbore ( $\dot{m}_g = \rho_g Q_g$ ),  $\forall^t$  is the volume of gas at time  $t$ ,  $Q_{in}$  and  $Q_{out}$  are the volume flow rates of drilling fluid that approach and leave the well bottom, respectively. This equation reveals that the pressure rises with the increase of mass and reduction of volume of gas within the wellbore. Changes of mass and volume flow rates are averaged within a  $2\Delta t$  time-step in order to comply with the time-step used by the Method of Characteristics.

The volume flow rates that approach and leave the wellbore bottom at time  $t + 2\Delta t$  are computed by using  $V_{p,1}^{t+2\Delta t}$  and  $V_{a,1}^{t+2\Delta t}$  and the cross section area  $A_s$  ( $Q = VA_s$ ). Therefore, the unknowns of Eqs. (6), (9), (10) and (11) are the pressures,  $P_w$ ,  $P_{p,1}$ ,  $P_{a,1}$  and  $P_g^{t+2\Delta t}$ , the gas flow rate  $Q_g$ , and the velocities,  $V_{p,1}^{t+2\Delta t}$  and  $V_{a,1}^{t+2\Delta t}$ . By assuming that the pressure in both annular region and drillpipe at the wellbore bottom are equal to the pressure of the gas, a system of four unknowns and four equations can be solved. A second order algebraic equation can then be found for the pressure at the wellbore bottom. By considering a known initial condition, the set of equations (7) and (8) together with the second order equation for the pressure at the wellbore bottom can be solved for evaluation of velocity and pressure along the whole domain at each time-step.

## 2.4 Initial and boundary conditions

A steady-state flow condition is assumed as the problem initial condition,  $Q(z, t=0) = Q_0$ , so that the stabilized pressure along the well is a function of the flow rate,  $P(z, t=0) = f(Q_0, z)$ . At time zero, the drillbit reaches a formation region in which the pore pressure is higher than the inside well pressure.

At the simulation start-up, the pump constant flow rate is considered as the inlet boundary condition whereas, a constant pressure is assumed at the outlet once the well is open to atmosphere. As soon as the kick has been detected, the pump is switched off and the well is closed. At this time, a zero flow rate is assumed for both inlet and outlet and the boundary pressures will then be calculated at each time-step.

## 3. RESULTS

In this section, the results of the simulation of a kick of gas are analyzed. For this first work, the gas properties are assumed to be identical to those of the air that is considered ideal even for high pressures. Firstly, changes of pressure of a typical problem are presented and discussed and secondly, a sensitivity analysis regarding the reservoir permeability, the fluid viscosity and the time for closing the well is conducted.

Table 1. Parameters used in the simulations.

<b>Geometry</b>	Well Depth (Annular and pipe lengths)	4300 m
	Drillpipe inside diameter	0.112 m (4.4")
	Drillpipe outside diameter	0.127 m (5.0")
	Diameter of the Well	0.216 m (8.5")
<b>Drilling fluid</b>	Density	1270.2 kg/m <sup>3</sup> (10.6 ppg)
	Viscosity	0.050 Pa.s (50 cP)
	Wave speed / isothermal compressibility	1254.8 m/s / $5 \times 10^{-10} \text{ Pa}^{-1}$
<b>Pumping parameters</b>	Drilling fluid flow rate	0.0063 m <sup>3</sup> /s (100 gpm)
	Time for well closure	50 s
<b>Influx parameters</b>	Air density (at reservoir)	441.6 kg/m <sup>3</sup>
	Gas constant (for air)	286.9 J/kgK
	Reservoir pressure	56.26 MPa
	Reservoir permeability to gas	$10^{-13} \text{ m}^2$
	Gas temperature at well bottom	50°C (323 K)
<b>Simulation parameters</b>	Finite volume length	5.06 m (N=1700)
	Time-step	4.03 ms
	Gravity acceleration	9.81 m/s <sup>2</sup>

### 3.1 Case study

The employed parameters for the case study are depicted in Tab. 1. These data represents as close as possible a typical case found in some phase of drilling operations. For all cases, the pumping system is turned off and the well is closed after 50 seconds. The reservoir pressure is considered to be 5% larger than hydrostatic pressure at the well bottom and the reservoir permeability is assumed to be  $10^{-13} \text{ m}^2$ . As the gas injection is assumed to take place in a concentrated point near the well bottom, the relation  $A_r/\mu_g L_r$  in Eq. (6) is assumed to be constant and equal to 27000.

The hydrostatic pressure is assumed to increase linearly from zero to 53.58 MPa at the well bottom that is 4300 m deep. The pump flow rate of  $0.0063 \text{ m}^3/\text{s}$  (100 gpm) causes a total pressure drop of 0.69 MPa so that the initial pressure at the well bottom is only 0.34 MPa higher than the hydrostatic pressure.

The kick start-up takes place at  $t=0$  when the gas begins to enter the wellbore. As the reservoir-to-wellbore pressure difference is high at the start-up, the gas influx is initially large. Fig. 3 shows the time evolution of the inlet gas flow rate and the volume occupied by the gas at the well bottom during the kick. As noted, the initial gas flow rate reduces with the pressure increase at the borehole up to 6.8 s when there is a slight growth followed by a further reduction up to 13.7 s. After that, the flow rate rises again up to 20.6 seconds. After that the mass flow rate stays almost constant until 53.4 s (3.4 s after the well has been closed) and then starts to decrease. The reduction takes place slowly reaching a zero flow rate when the inside well pressure matches the reservoir pressure. The volume occupied by the gas at the wellbore depends on the mass of gas so that a high gas expansion takes place before closing the well. The gas flow rate oscillations are related to pressure wave propagation and reflection. The wave takes approximately 3.4 s to cross the 4300 m of well length. With the gas influx, two pressure waves are produced; one that propagates through the drillpipe and the other through the annular space. They both reach the surface in 3.4 s and are reflected to the well bottom. At 6.8 s, the waves meet each other and are superposed, reducing immediately the pressure at the well bottom and consequently, increasing the influx of gas.

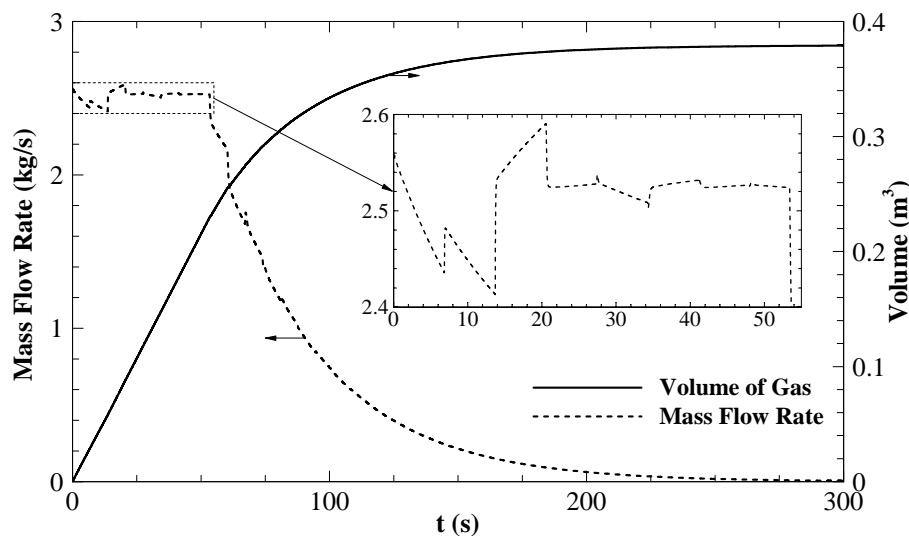


Figure 3. Time change of gas flow rate and volume occupied by the gas at the borehole.

Because of pressure propagation and gas expansion within the well, the pressure distribution is subjected to fluctuations along the well length. Fig. 4 shows pressure changes above hydrostatic pressure at the drillpipe inlet, at the annular space outlet and at well bottom. As can be seen, the gas influx causes a significant pressure variation that are mainly related to pressure propagation and reflection. The inlet pressure that is 0.69 MPa at the start-up undergoes a sudden growth to 1.05 MPa at 3.4 s. The pressure at the well bottom is directly related to the mass, temperature and volume of gas. The pressure at the annular outlet is set to zero as boundary condition before closing the well. Nevertheless, the annular outlet pressure rises instantaneously with the well closure at 50s. As soon as the pump is turned off and the well is closed down, the source of pressurization is removed and drillpipe inlet pressure drops. After successive pressure reflections with the well closed, the well bottom pressure is balanced by the reservoir pressure and the pressure along the well increases approximately 2.68 MPa. In other words, it grows from 53.58 to 56.26 MPa. The 300 s shown in Fig. 4 is not enough to reach this final value.

With the gradual increase of gas volume within the well, the drilling fluid is displaced and oscillations of flow rate take place in the drillpipe and annular space. Fig. 5 depicts changes of volume flow rate in three positions: annular outlet and both annular space and drillpipe at the well bottom. As noted, the drilling fluid circulates with a constant initial flow rate of  $0.0063 \text{ m}^3/\text{s}$  when the kick takes place and the drilling fluid is suddenly accelerated in the annular space and refrained in the drillpipe. Whereas the flow rates increases oscillating in the annular space, it fluctuates

around the initial flow rate in the drillpipe. As soon as the well is closed, the flow rates are reduced and oscillate around zero until the well pressure is balanced by the reservoir pressure. As shown, the flow rates drop to zero after 120 s.

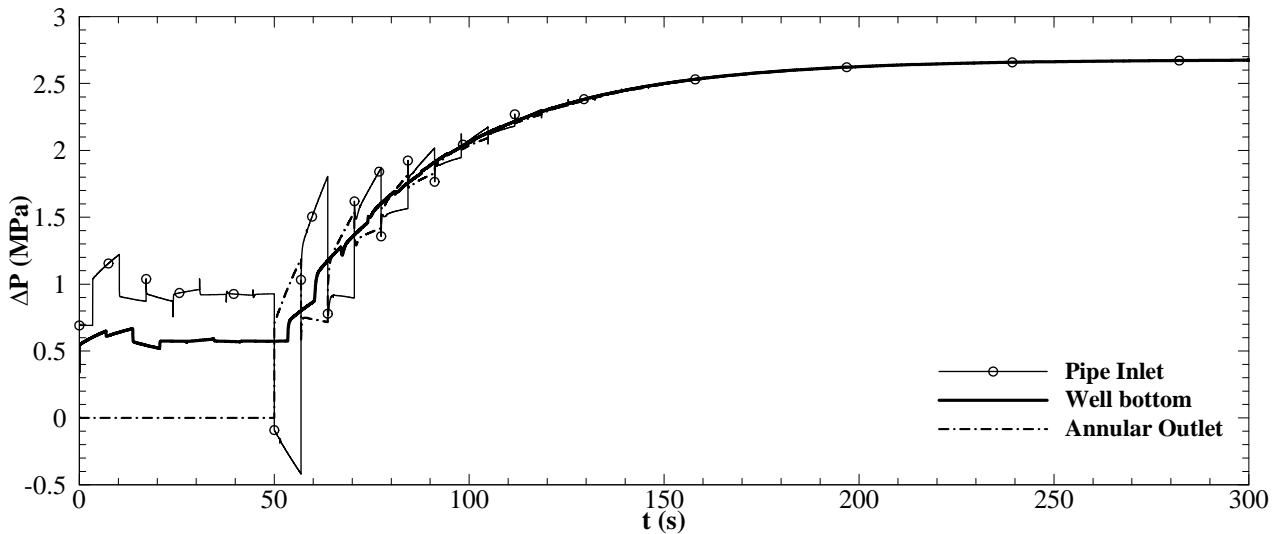


Figure 4. Time change of pressure at drillpipe inlet, at the well bottom and at the annular outlet after a gas influx.

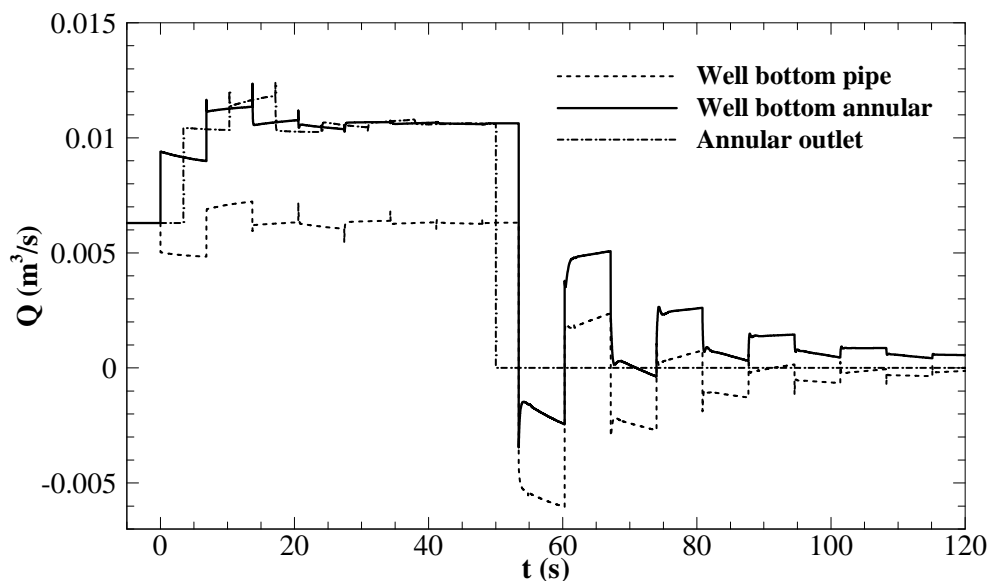


Figure 5. Time change of volume flow rates in different well positions.

### 3.2 Sensitivity analysis

For the current mathematical model, a sensitivity analysis regarding reservoir permeability, fluid viscosity and time for well closing was performed. The situation shown in Tab. 1 was considered as a reference case and each parameter was changed one each a time.

#### 3.2.1 The effect of permeability

The effect of well permeability in the borehole bottom pressure and gas volume within the well is now investigated. The values used for the permeability were  $10^{-14}$  m<sup>2</sup>,  $10^{-13}$  m<sup>2</sup> and  $10^{-12}$  m<sup>2</sup>, whereas the ratio  $A_r/\mu_g L_r$  was kept equal to 27000 for all cases. Fig. 6 illustrates the changes of wellbore bottom pressure after a kick for the different values of permeability. The higher the permeability the higher is the initial pressure rise, as the gas flow rate increases with the

permeability according to the Darcy's law. After the well has been closed, all cases stabilize in the same pressure independently of the permeability value. Nevertheless, the higher the permeability the lower is the stabilization time.

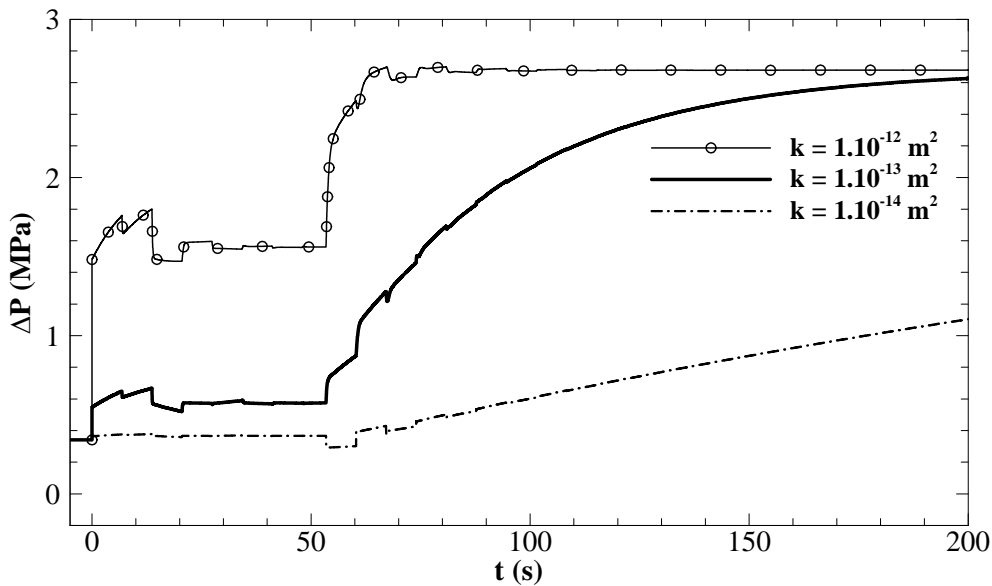


Figure 6. Time change of well bottom pressure after the kick for different reservoir permeability.

As shown in Fig. 7, not only the gas volume in the wellbore increases with the permeability but also the gas volume flow rate. The final gas volume within the wellbore is in the order of  $1.22 \text{ m}^3$  for a permeability of  $10^{-12} \text{ m}^2$ , whereas it is  $0.38 \text{ m}^3$  and  $0.17 \text{ m}^3$  for  $10^{-13} \text{ m}^2$  and  $10^{-14} \text{ m}^2$ , respectively.

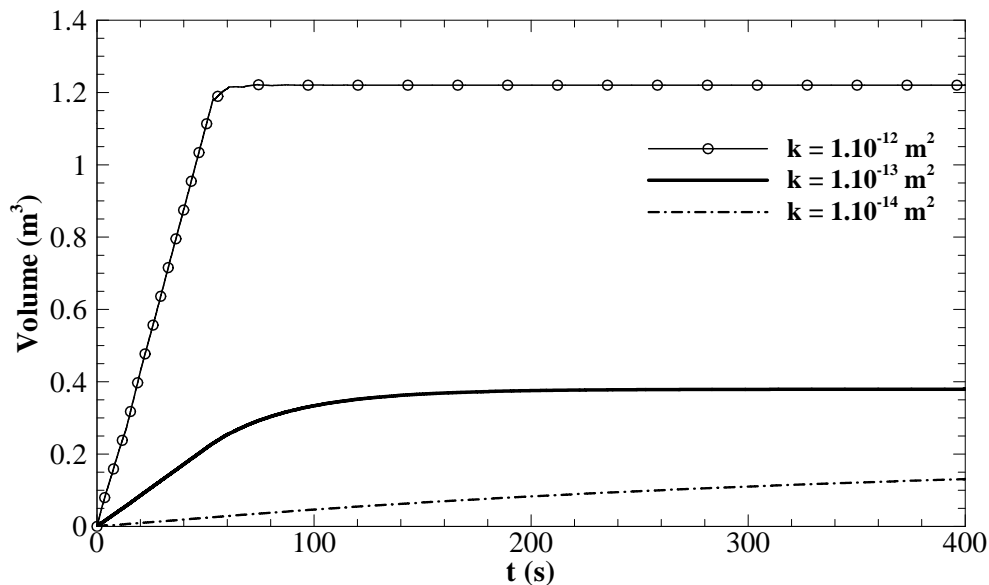


Figure 7. Time change of gas volume within the wellbore after a kick for different reservoir permeability.

### 3.2.2 The effect of fluid viscosity

High fluid viscosity requires high pumping pressure for a constant volume flow rate. Fig. 8 shows the pressure change after the kick for two fluid viscosities. The final pressure is reached firstly for the higher viscosity fluid because the initial pressure within the wellbore is higher for larger viscosity fluids. For a viscosity of  $0.05 \text{ Pa}\cdot\text{s}$ , the well bottom pressure is  $0.34 \text{ MPa}$  higher than the hydrostatic pressure, whereas for a viscosity of  $0.1 \text{ Pa}\cdot\text{s}$  it is  $0.68 \text{ MPa}$ . It is noteworthy that the pressure does not drop after pressure superposition at  $6.8 \text{ s}$  at well bottom for the higher viscosity fluid because of the higher dissipation of the pressure wave.



Fig. 9 depicts the pressure change at the annular outlet after closing the well at 50 s. As shown, the higher viscosity fluid undermines the magnitude of pressure fluctuations.

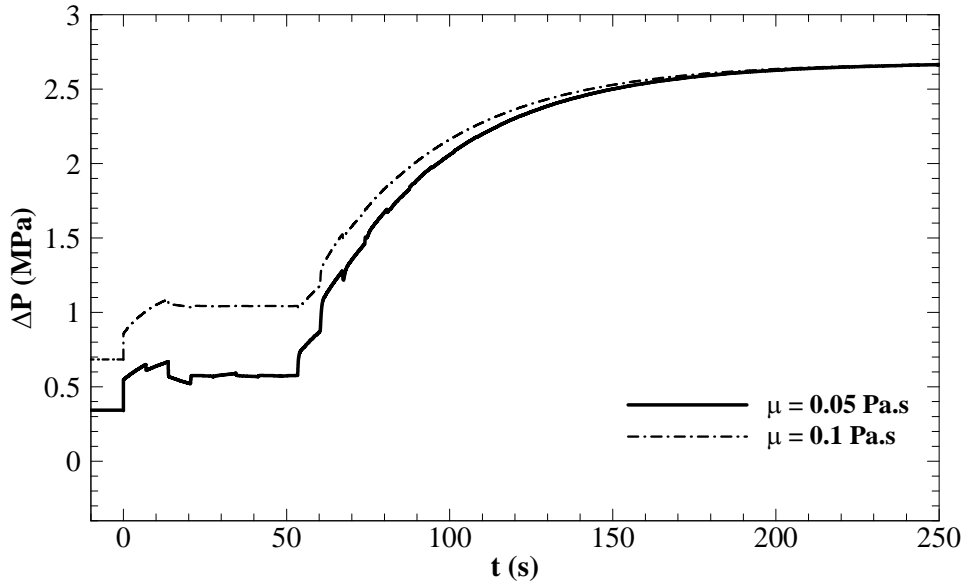


Figure 8. Time change of well bottom pressure after a kick for different viscosity fluids.

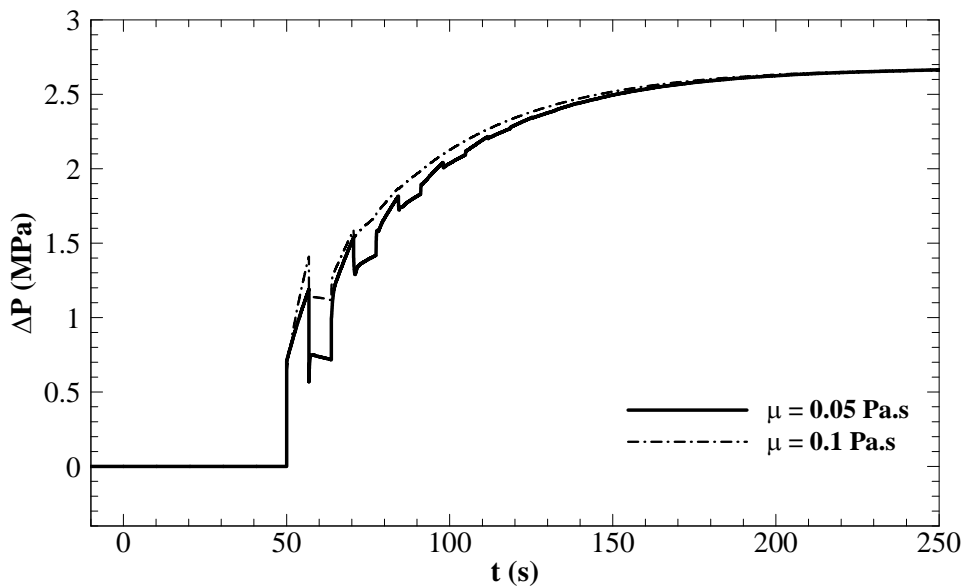


Figure 9. Time change of annular pressure after a kick for different viscosity fluids.

### 3.2.3 The effect of the well closing time

The time for closing the well after a kick is a quite important parameter. Two different well closing times are now investigated. Fig. 10 shows the time change of pressure at the well bottom for closing times of 50 and 100 seconds, respectively. After the initial pressure change, the pressure tends to stabilize as the ratio of mass and volume of gas becomes constant. When the well is closed, there is a sudden change of the problem boundary conditions and the well bottom pressure increases again to reach the steady-state.

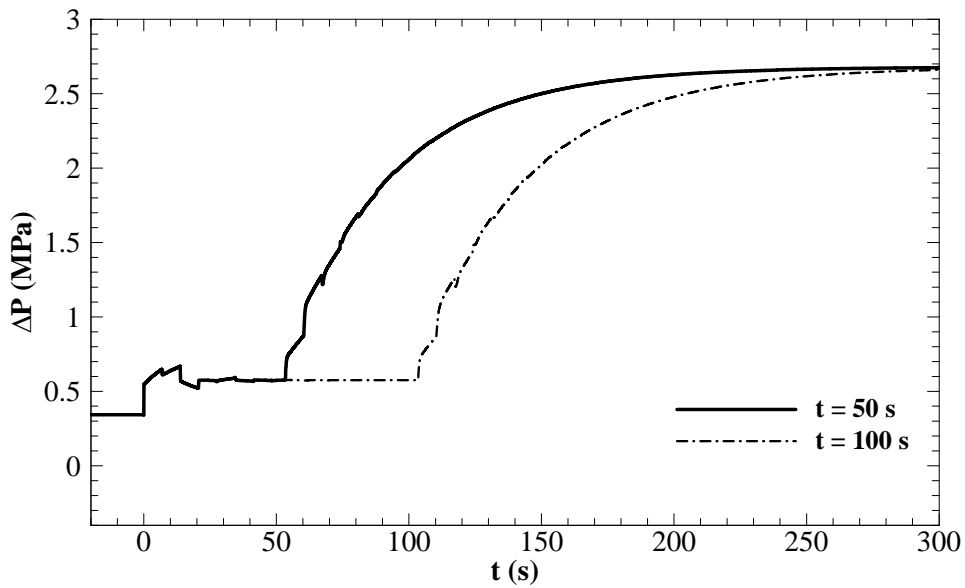


Figure 10. Time change of well bottom pressure after a kick for two different well closing times.

As depicted in Fig. 11, the pressure at the annular outlet changes similarly to the pressure at the well bottom. As this pressure variation is related to flow inertia,  $\Delta P \sim \rho cV$ , and the drilling fluid flow rate is almost at steady-state after 50 s (see Fig. 5), the pressure changes will be very similar.

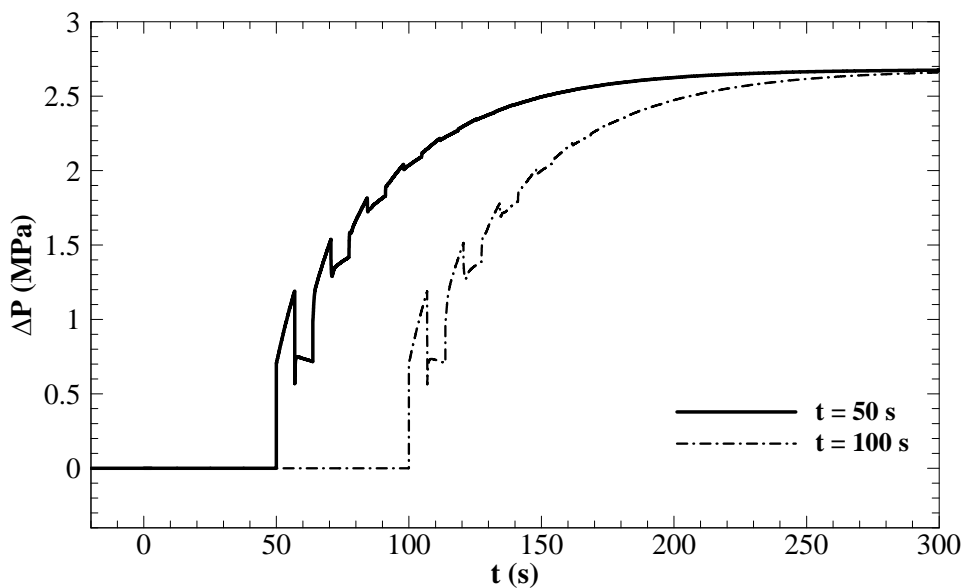


Figure 11. Time change of pressure at the annular outlet after a kick for two different well closing times.

Figure 12 shows the time change of gas volume within the wellbore for both cases. As already discussed, the gas expansion is larger before than after closing the well and therefore, the higher the closing time the larger is the amount of gas that enters the well. As noted, the gas volume after 300 s is  $0.59 \text{ m}^3$  for a closing time of 100 s whereas, it is smaller than  $0.4 \text{ m}^3$  for a closing time of 50 s.

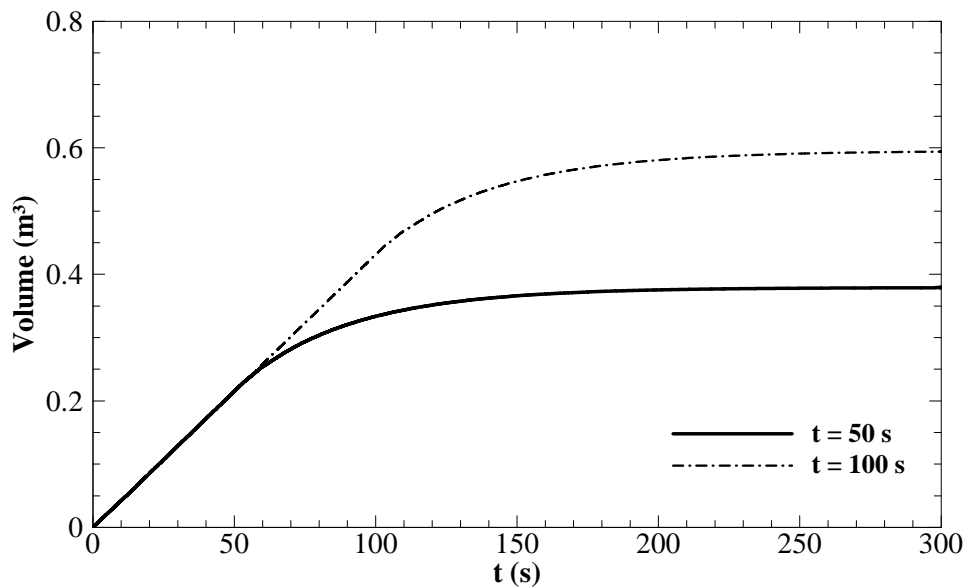


Figure 12. Time change of volume of gas within the wellbore after a kick for two different well closing times.

#### 4. CONCLUSIONS

A mathematical model for evaluation of the pressure propagation and flow rates after kick of gas was presented in the current work. The model is based on the conservation equations of mass and momentum for one-dimensional, compressible and transient flows. In this first study, the drilling fluid was considered Newtonian, the gas was dealt as ideal, migration and dissolution of gas were disregarded and the process is admitted isothermal. The influx of gas that is dependent on the reservoir pressure and reservoir permeability to gas was computed by using the Darcy's law.

A case study revealed that the pressure begins to propagate as soon as the influx of gas starts causing pressure and flow rates oscillations within the wellbore as pressure reflects and is superposed at well ends. The pressure changes at the borehole bottom takes some time to be sensed at the well surface as the pressure propagates at finite and known speed.

A sensitivity analysis was conducted to show that:

- i) the higher the amount of gas that enters the well, the higher the pressure variations and the amount of drilling fluid that returns to the surface;
- ii) enlarging the rock permeability not only is the influx of gas to the wellbore increased but also the pressure variation at the well bottom and at the annular outlet;
- iii) high viscous flows reduce pressure peaks and stabilize faster the pressures within the well, as viscous dissipation and initial bottomhole pressures are higher;
- iv) the volume of gas that invades the well is significantly dependent on the time for closing the well.

As the results of this first study are quite encouraging, future works must be conducted so as to deal the drilling fluid as viscoplastic, the gas as non-ideal and with the migration and dissolution of gas in the drilling fluid.

#### 5. ACKNOWLEDGEMENTS

The authors acknowledge the financial support of PETROBRAS S/A, ANP (Brazilian National Oil Agency) and CNPq (The Brazilian National Council for Scientific and Technological Development).

#### 6. REFERENCES

- Avelar, C.S., Ribeiro, P.R. and Sepehrnoori, K., 2009. "Deepwater gas kick simulation". *Journal of Petroleum Science and Engineering*. Vol. 67, p. 13–22.
- Cawkwell, M.G. and Charles, M.E., 1987. "An improved model for start-up of pipelines containing gelled crude oil". *J. Pipelines*, Vol. 7, p. 41–52.

J. F. Galdino, G. M. Oliveira, A. T. Franco and C. O. R. Negrão  
 Transient Mathematical Model For Well Kick During Drilling Operations

- Chang, C., Rønningsen, H.P. and Nguyen, Q.D., 1999. "Isothermal start-up of pipeline transporting waxy crude oil". *J. Non-Newtonian Fluid Mech*, Vol. 87, p. 127–154.
- Davidson, M.R., Nguyen, Q.D., Chang, C. and Rønningsen, H.P., 2004. "A model for restart of a pipeline with compressible gelled waxy crude oil". *J. Non-Newtonian Fluid Mech*, Vol. 123, p. 269–280.
- El-Gendy, H., Alcoutlabi, M., Jemmett, M., Deo, M., Magda, J., Venkatesan, R. and Montesi, A., 2012. "The propagation of pressure in a gelled waxy oil pipeline as studied by particle imaging velocimetry". *AIChE J*, Vol. 58 (1), p. 302–311.
- Hoferock, L.L. and Stanbery, S.R., 1981. "Pressure Dynamics in Wells During Gas Kicks: Part 2 - Component Models and Results". *Journal of Petroleum Technology*, Vol. 33, p. 1367–1378.
- Lage, A.C.V.M., 1990. *Simulação e controle de poços de petróleo em erupção* (in portuguese). M.Sc dissertation, COPPE, Universidade Federal do Rio de Janeiro, Rio de Janeiro.
- LeBlanc, J.L. and Lewis, R.L., 1968. "A Mathematical Model of a Gas Kick". *Journal of Petroleum Technology*, Vol. 103, p. 888–898.
- Negrão, A.F., 1989. *Controle de poço em águas profundas* (in portuguese). M.Sc dissertation, Faculdade de Engenharia Mecânica, Universidade Estadual de Campinas, Campinas.
- Negrão, C.O.R., Franco, A.T. and Rocha, L.L.V., 2011. "A weakly compressible flow model for the restart of thixotropic drilling fluids". *J. Non-Newtonian Fluid Mech*, Vol. 166, p. 1369–1381.
- Nickens, H., 1987. "A dynamic computer model of a kicking well". *SPE Drilling Engineering*, Vol. 2, p. 158–173.
- Nield, D. A. and Bejan, A., 2013. *Convection in Porous Media*. Springer; 4<sup>th</sup> edition.
- Nickens, H.V., 1987. "A dynamic computer model of a kicking well". *SPE Drilling Engineering*, Vol. 2, p. 158–173.
- Nunes, J.O.L., 2001. *Estudo do controle de poços em operações de perfuração em águas profundas e ultra profundas* (in portuguese). M.Sc dissertation, Faculdade de Engenharia Mecânica, Universidade Estadual de Campinas, Campinas.
- Nunes, J.O.L., Bannwart, A.C. and Ribeiro, P.R., 2002. "Mathematical Modeling of Gas Kicks in Deep Water Scenario". In *Proceedings of the IADC/SPE Asia Pacific Drilling Technology* 8-11 September. Jakarta, Indonesia.
- Ohara, S., 1995. *Improved method for selecting kick tolerance during deepwater drilling operations*. Ph.D. thesis, Louisiana State University, Baton Rouge.
- Oliveira, G.M., Rocha, L.L.V., Franco, A.T. and Negrão, C.O.R., 2010. "Numerical simulation of the start-up of Bingham fluid flows in pipelines". *J. Non-Newtonian Fluid Mech*, Vol. 165, p. 1114–1128.
- Oliveira, G.M., Franco A.T., Negrão C.O.R., Martins, A.L. and Silva, R.A., 2013. "Modeling and validation of pressure propagation in drilling fluids pumped into a closed well". *Journal of Petroleum Science and Engineering*, Vol. 103, p. 61–71.
- Records, L.R., 1972. "Mud system and well control". *Petroleum Engineering*, Vol. 44, p. 97–108.
- Santos, O.L.A., 1982. *A mathematical model of a gas kick when drilling in deep waters*. M.Sc dissertation, Colorado School of Mines, Golden.
- Stanbery, S.R., 1976. *Well pressure dynamics under impending blowout conditions*. Ph.D. thesis, University of Texas at Austin, Austin.
- Sestak, J., Cawkwell, M.G., Charles, M.E. and Houskas, M., 1987. "Start-up of gelled crude oil pipelines". *J. Pipelines*, Vol. 6, p. 15–24.
- Vinay, G., Wachs, A. and Agassant, J.F., 2006. "Numerical simulation of weakly compressible Bingham flows: the restart of pipeline flows of waxy crude oils". *J. Non-Newtonian Fluid Mech*, Vol. 136 (2–3), p. 93–105.
- Vinay, G., Wachs, A. and Frigaard, I., 2007. "Start-up transients and efficient computation of isothermal waxy crude oil flows". *J. Non-Newtonian Fluid Mech*, Vol. 143, p. 141–156.
- Wachs, A., Vinay, G. and Frigaard, I., 2009. "A 1.5D numerical model for the start up of weakly compressible flow of a viscoplastic and thixotropic fluid in pipelines". *J. Non-Newtonian Fluid Mech*, Vol. 159, p. 81–94.
- White, F.M., 2003. *Fluid Mechanics*. McGraw-Hill, New York, 5<sup>th</sup> edition.
- Wylie, E. B., Streeter, V. L. and Suo, L., 1993, *Fluid Transients in Systems*. Prentice Hall, New Jersey, 1<sup>st</sup> edition.

## 7. RESPONSIBILITY NOTICE

The authors are the only responsible for the printed material included in this paper.